Photosynthesis Research **48**: 227–237, 1996.

Regular paper

EPR and ENDOR studies of the water oxidizing complex of Photosystem II

Robert Fiege[1], Wolfgang Zweygart[1], Robert Bittl[1], Noam Adir[2], Gernot Renger[1] & Wolfgang Lubitz[1,*]

[1]*Max-Volmer-Institut für Biophysikalische und Physikalische Chemie, Technische Universität Berlin, Str. des 17. Juni 135, D-10623 Berlin, Germany;* [2]*Department of Physics, University of California, San Diego, La Jolla, CA. 92093-0319, USA;* **Author for correspondence and reprint requests*

Received 2 November 1995; accepted in revised form 9 January 1996

Key words: manganese cluster, multiline signal, oxygen evolution, S-states, water ligation

Abstract

A comparative study of X-band EPR and ENDOR of the S_2 state of photosystem II membrane fragments and core complexes in the frozen state is presented. The S_2 state was generated either by continuous illumination at T = 200 K or by a single turn-over light flash at T = 273 K yielding entirely the same S_2 state EPR signals at 10 K. In membrane fragments and core complex preparations both the multiline and the g = 4.1 signals were detected with comparable relative intensity. The absence of the 17 and 23 kDa proteins in the core complex preparation has no effect on the appearance of the EPR signals. ^{1}H-ENDOR experiments performed at two different field positions of the S_2 state multiline signal of core complexes permitted the resolution of four hyperfine (hf) splittings. The hf coupling constants obtained are 4.0, 2.3, 1.1 and 0.6 MHz, in good agreement with results that were previously reported (Tang et al. (1993) J Am Chem Soc 115: 2382–2389). The intensities of all four line pairs belonging to these hf couplings are diminished in D_2O. A novel model is presented and on the basis of the two largest hfc's distances between the manganese ions and the exchangeable protons are deduced. The interpretation of the ENDOR data indicates that these hf couplings might arise from water which is directly ligated to the manganese of the water oxidizing complex in redox state S_2.

Abbreviations: cw – continuous wave; ENDOR – electron nuclear double resonance; EPR – electron paramagnetic resonance; hf – hyperfine; hfc – hyperfine coupling; MLS – multiline signal; PS II – Photosystem II; rf – radio frequency; WOC – water oxidizing complex

Introduction

Photosynthetic water oxidation to molecular oxygen and the coupled release of four protons take place within a manganese containing functional unit referred to as water oxidizing complex (WOC). The overall process comprises a sequence of four univalent electron transfer steps that is designated as the Kok-cycle. The redox states of the WOC are symbolized by S_i where i = 0...4, the index i represents the number of oxidizing equivalents above the redox level formally corresponding to that of substrate water. This highly endergonic reaction sequence is energetically driven by $P_{680}^{+\bullet}$, the oxidant which is formed during the primary step of light induced charge separation within the PS II reaction center (for a review see Renger 1992). A redox active tyrosine residue of polypeptide D1 (symbolized by Y_Z and identified by Debus et al. 1988a and Metz et al. 1989) acts as intermediate electron carrier in the process of stepwise electron abstraction from the WOC by $P_{680}^{+\bullet}$. In addition to the main oxidative pathway via Y_Z, the WOC in its different redox states S_i can also interact with other endogenous redox groups. Among them, a tyrosine located in polypeptide D2 (Debus et al. 1988b; Vermaas et al. 1988) and symbolized by Y_D is in redox equilibrium with the S-states of the WOC

possibly comprising the redox couples P_{680}/P_{680}^{+} and Y_Z/Y_Z^{ox} (Messinger et al. 1993; Messinger and Renger 1993). Accordingly, Y_D^{ox} contributes to the cw EPR signal of PS II preparations, while Y_Z^{ox} can be monitored only at sufficient time resolution due to its fast turnover kinetics.

Although detailed information is available on the kinetic pattern of the Kok cycle (for reviews see Babcock 1987, Renger 1987 and Debus 1992) key questions are still not answered with respect to i) the electronic structure and nuclear geometry of the WOC in the different redox states S_i and ii) the mechanism(s) of water oxidation (discussed in Renger 1987, 1993).

In principle, magnetic resonance methods should provide powerful tools to address both questions. Information on the electronic structure of the manganese cluster is expected to be obtainable by EPR. In practice, however, several complications arise. First, EPR signals of a functionally competent WOC could be only observed for the redox state S_2 (first observed by Dismukes and Siderer 1980, for a review see Miller and Brudvig 1991). Secondly, the interpretation of the EPR spectrum of the S_2 state – characterized by a g = 4.1 signal and a highly structured multiline signal (MLS) around g = 2 – is difficult because of the complex spin coupling in manganese clusters. Therefore, the origin of these signals is a matter of debate (de Paula et al. 1987; Pace et al. 1991) although agreement exists on the dominating contribution of a mixed valent Mn(III) Mn(IV) group leading to a $S_{eff} = 1/2$ ground state (Britt et al. 1992; Bonvoisin et al. 1992; Åhrling and Pace 1995).

A full understanding of the complex MLS has, however, not been achieved so far. The number of lines and the spectral width has been explained by coupling of all four Mn in the cluster (Bonvoisin et al. 1992; Kusunoki 1992; Zheng and Dismukes 1992) or by only two Mn (Åhrling and Pace 1995). In the approach of Bonvoisin et al. (1992) and of Kusonoki (1992) only isotropic hf interactions of the manganese were assumed. In contrast, Åhrling and Pace (1995) used two strongly anisotropic hf tensors for Mn(III) and Mn(IV) and a large contribution from the Mn quadrupole interaction had to be included in the simulations.

The interaction with ligands – including substrate water molecules – can be analyzed by ENDOR measurements. A complication is, however, the limited sensitivity of ENDOR and the possibility of contributions from EPR signals that occur in the same spectral region and that are generated by redox reactions of functional groups *other* than the manganese cluster (e.g. Y_D^{ox}, Cytochrome b-559, iron quinone $FeQ_A^{-\bullet}$).

In the present paper, we compare EPR signals of dark adapted (WOC in redox state S_1) and illuminated (WOC in S_2) PS II membrane fragments and core complexes of higher plants (spinach). We show that the multiline and g = 4.1 S_2 state signals are virtually the same and that differences in the appearance of the spectra are not related to the WOC. Furthermore, ENDOR signals obtained from the MLS are reported for PS II core complexes. These signals are compared with those obtained in earlier studies by our group (Zweygart et al. 1992) and other laboratories (Kawamori et al. 1989; Tang et al. 1993). The study of Khangulov et al. (1993) presents a model that allows the evaluation of effective hyperfine couplings along the magnatic field axis for the Mn(III)Mn(IV) complex in catalase. This model has been applied to the WOC by Tang et al. (1993) to estimate possible manganese proton distances. Based on these general ideas, an extended model is proposed that takes into account the spin-spin coupling of a Mn(III)Mn(IV) dimer and the possibility of non-axial hf tensors thereby leading to modified proton manganese distances in the S_2 state of the WOC.

Materials and methods

Sample preparation

PS II membrane fragments were isolated according to the procedure of Berthold et al. (1981) as modified by Völker et al. (1985). Light saturated rates of oxygen evolution and the oxygen yields per flash were measured with a Clark-electrode in suspensions containing the sample in buffer A (50 mM MES-NaOH, pH 6.5, 15 mM NaCl, 5 mM $MgCl_2$, 400 mM sucrose) and either $K_3[Fe(CN)_6]$/PPBQ (phenyl-p-benzoquinone) (final concentration, 1 mM/0.2 mM) or 2,6-DCBQ (dichlorobenzoquinone) (final concentration, 0.5 mM) as electron acceptors (Haag et al. 1990). The PS II membrane fragments revealed oxygen evolution rates of 400 ± 50 μmol O_2/mg Chl h.

PS II core complexes have been purified from spinach as described by Adir et al. (1992). The oxygen evolution rate was estimated in the presence of 2,6-DCBQ as electron acceptor and was in the range of 500–1000 μmol O_2/mg Chl h depending on the preparation. The PS II preparations were suspended in buffer B (50 mM MES-NaOH, pH 6.5, 15 mM NaCl,

5 mM $MgCl_2$, 400 mM mannitol) using concentrations of 10 mg Chl/ml for membrane fragments and 4 mg Chl/ml for core complexes. This is equivalent to a reaction center concentration of 50 μM for membrane fragments and of 150 μM for core complexes.

EPR and ENDOR experiments

For EPR and ENDOR measurements, the samples were placed in oxygen-free argon flushed quartz tubes (3 mm inner diameter). Two different techniques have been used to generate the S_2 state: the sample was either (i) continuously illuminated at 200K inside the EPR cavity by a 150 W halogen lamp connected to the EPR resonator by fiber optics, or (ii) irradiated at 273 K by a single turn-over light flash from a Xe lamp and then trapped by freezing.

The EPR spectra were recorded on a Bruker ESP 300E or on a Varian E-9 spectrometer using a standard Bruker TE_{102} cavity with an Oxford ESR 9 cryostat (4.2–300 K). For the ENDOR measurements, a home-built high sensitivity TM_{110} cavity (Zweygart et al. 1994) attached to an Oxford ESR 910 cryostat (1.9–300 K) was used. The cryostat was controlled by an Oxford ITC4 temperature unit. The radio frequency was generated by a Rohde & Schwarz rf synthesizer (SMG), amplified by an ENI solid state amplifier (A200L) and terminated by a 50 Ω load.

ENDOR data analysis

In ENDOR spectra of isotropic samples two lines appear for each magnetic nucleus spaced, to first order, symmetrically around the nuclear Larmor frequency ν_n. These lines are separated by the respective isotropic hyperfine coupling constant (hfc) a (for protons with $\nu_H > a/2$). The ^{1}H-ENDOR frequencies are given by (Kurreck et al. 1988):

$$\nu^{\pm}_{ENDOR} = |\nu_H \pm a/2|. \quad (1)$$

For randomly oriented molecules, in powders or frozen solutions, one obtains pronounced features in the solid state ENDOR spectrum corresponding to the inflection points of the absorption spectrum. For axially symmetric hf tensors, with small anisotropy, usually both principal values $A_{||}$ and $A_{\perp}$ can be obtained. The signals have characteristic line shapes and the hf tensor principal components are related to each other by $A_{||} = -2A_{\perp}$. In the case of a purely dipolar hf tensor, e.g. a hydrogen bond proton, the length r of the respective hydrogen bond given in Å can be estimated by using the simple point-dipole approximation:

$$A(\theta) = \frac{c}{r^3}\rho(3\cos^2\theta - 1), \quad (2)$$

where $A(\theta)$ is the hf coupling in MHz, $c = g_e\mu_e g_n\mu_n$ and equals 79 MHzÅ^3 for a proton, ρ is the unpaired electron spin density, θ is the angle between the applied magnetic field B_0 and the vector connecting the electron and the proton.

The interpretation of ENDOR spectra of coupled metal clusters is further complicated by the fact that, even under the assumption of a point-dipole model, hyperfine coupling tensors of the ligand protons are not necessarily axial. In the following the situation for a magnetically coupled dimanganese Mn(III)Mn(IV) complex is described. The outlined ideas can also be extended to three or four manganese nuclei. The hyperfine coupling of a proton to a Mn(III)Mn(IV) complex can formally be desribed by the hamiltonian

$$\mathcal{H} = \underline{I}_H \underline{\underline{a}}^1_H \underline{S}_1 + \underline{I}_H \underline{\underline{a}}^2_H \underline{S}_2; \quad (3)$$

with $\underline{\underline{a}}^1_H$ and $\underline{\underline{a}}^2_H$ being the intrinsic hyperfine tensors for a proton coupled to a Mn(III) and to a Mn(IV), respectively. $\underline{I}_H$ is the nuclear spin of the proton and $\underline{S}_1$ and $\underline{S}_2$ are the spin operators of the electron spins. Using the point-dipole approximation the two tensors $\underline{\underline{a}}^i_H$, $i = 1,2$ are axial; however, they are in general diagonal in *different* coordinate systems. In magnetically coupled spin systems, an adequate representation of the hamiltonian Equation (3) is given by the effective spin S_{eff} instead of S_i, $i = 1,2$. For antiferromagnetically coupled Mn(III) and Mn(IV) with $S_{III} = 2$ and $S_{IV} = 3/2$, the total spin is $S_{eff} = 1/2$,

$$\mathcal{H} = \underline{I}_H \underline{\underline{A}}^S_H \underline{S}_{eff}, \text{ and} \quad (4)$$

$$\underline{\underline{A}}^S_H = c_1 \underline{\underline{a}}^1_H + c_2 \underline{\underline{a}}^2_H, \quad (5)$$

where $c_i = 2$ for Mn(III) and $c_i = -1$ for Mn(IV). A calculation of the coefficients c_i for four coupled manganese atoms is given e.g. by Bittl (1993). The linear combination Equation (5) of the two axial tensors $\underline{\underline{a}}^i_H$ with different principal axis system results, in general, in a non-axial tensor $\underline{\underline{A}}^S_H$. We use the inherent symmetry of the system, to calculate principal values of the tensor $\underline{\underline{A}}^S_H$ directly by

$$(A^S_H)_{ii} = c(-\delta,\ -\Gamma + \delta/2,\ \Gamma + \delta/2), \quad (6)$$

$$\delta = 2r_1^{-3} - r_2^{-3} \quad , \text{ and} \quad (7)$$

$$\Gamma = 3/2\sqrt{4r_1^{-6} - 4r_1^{-3}r_2^{-3}\cos 2\psi + r_2^{-6}}, \quad (8)$$

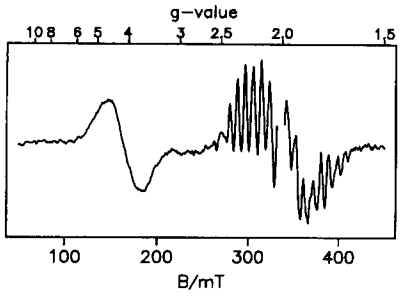

Figure 1. Light *minus* dark difference X-band EPR spectrum of PS II membrane fragments from spinach in buffer B (see text); the sample was illuminated at T = 200 K for 10 min and then cooled to cryogenic temperature; experimental conditions: microwave frequency 9.44 GHz, microwave power 10 mW, field modulation 2.0 mT_{pp}, temperature 10 K, recording time 30 min for the spectrum in the dark adapted state as well as after illumination.

where, the geometrical parameters r_i and ψ are defined in scheme 1 and c being the same as in Equation (2). The principal values of $\underline{\underline{A}}_H^S$ are observed as pronounced lines in an ENDOR experiment. Of the principal values given by Equation (6) the one corresponding to the largest statistical weight in a powder spectrum (central component) has the smallest absolute value. The expression for the hf tensor principal values $(A_H^S)_{ii}$ (Equation (6)) is simplified in the case characterized by $\psi = 0$ (scheme 2) as:

$$(A_H^S)_{ii} = c(2r_1^{-3} - r_2^{-3})(-1, -1, 2) \qquad (9)$$

that describes again an axial hf tensor. Note that for $\psi = 0$ all hyperfine components vanish simultaneously for $2r_1^{-3} - r_2^{-3} = 0$.

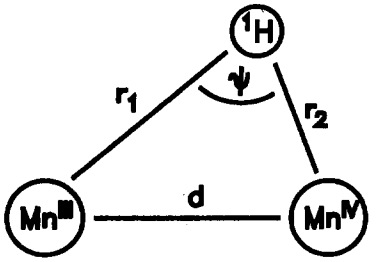

Scheme 1

Scheme 2

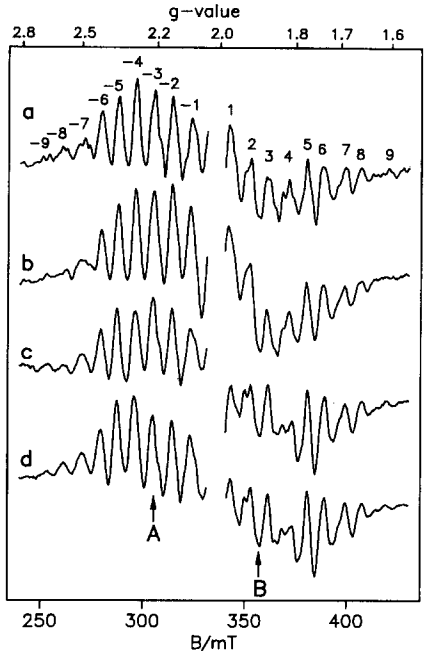

Figure 2. Light *minus* dark difference X-band EPR spectra of PS II membrane fragments (a, b) and PS II core complexes (c, d), both from spinach, in buffer B; the S_2 state was either flash-induced at T = 273 K (a, c) or generated by illumination at T = 200 K for 10 Min (b, d). In (a) the major lines are numbered with respect to the center near g = 2. Note that the central line is not shown. The total number of major lines is 19. In (d) the field positions are indicated (A, B) on which the ENDOR experiments have been performed; experimental conditions as in Figure 1.

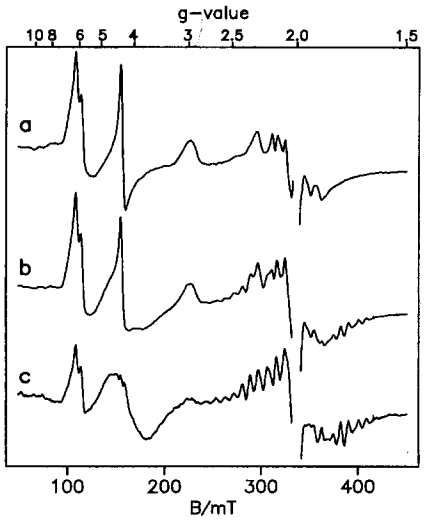

Figure 3. X-band EPR spectra of PS II core complexes (spinach) in buffer B; dark adapted state (a), after illumination at T = 200 K for 10 min (b) and the respective light *minus* dark difference spectrum (c); experimental conditions as in Figure 1; for further details see text.

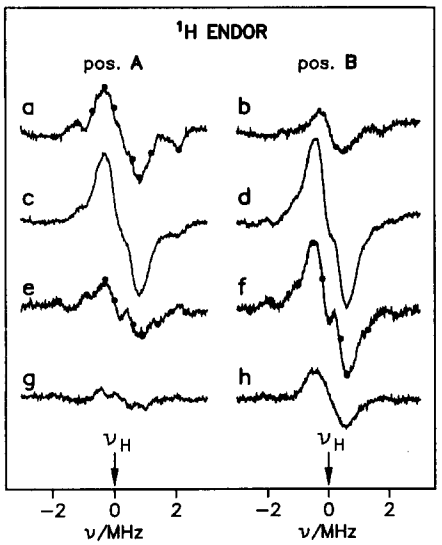

Figure 4. ^{1}H-ENDOR spectra of PS II core complexes (spinach) suspended in buffer B; the spectra were recorded at two different field positions, (A) at 298 mT that corresponds to g = 2.28 and (B) at 359 mT that corresponds to g = 1.89. The amplitudes of the signals are directly comparable. (a, b) spectra obtained from the dark adapted state; (c, d) after illumination at 200 K for 10 min; (e, f) light *minus* dark difference spectra representing the S_2 state signals; (g, h) light *minus* dark difference spectra of core complexes suspended in D_2O buffer. The line positions from which the hfc's are obtained are indicated by full circles (see a, e, f); experimental conditions: microwave frequency 9.5 GHz, microwave power 20 mW, rf power 150 W, frequency modulation 12.5 kHz with ± 100 kHz deviation, temperature 2 K, recording time 3 h for spectra from the dark adapted state and 6 h for spectra after illumination.

Results

EPR measurements

Figure 1 shows the X-band EPR signals (9.4 GHz) measured in suspensions of PS II membrane fragments induced by excitation of the dark adapted sample with continuous white light at T = 200K. At this temperature, the electron transfer from $Q_A^{-\bullet}$ to Q_B is blocked (Joliot and Joliot 1973; Koike and Inoue 1987; Renger et al. 1993) and PS II is limited to a single charge separation. The spectrum shown is a light *minus* dark difference spectrum. It exhibits the characteristic features of the water oxidase in redox state S_2, i.e. the broad g = 4.1 signal (peak to peak width 35 mT) and the multiline signal (MLS) centered at g ≅ 2 (for a review see Miller and Brudvig 1991). The signal of Y_D^{ox} appears at g = 2.0046. It is larger in amplitude than all other signals by more than one order of magnitude and is therefore omitted in the figure. In addition, a further light induced signal is superimposed on the high field region of the MLS and is ascribed to the reduced iron quinone complex ($Fe^{2+}Q_A^{-\bullet}$). The EPR signal of this species is known to lie between g = 1.8 and 1.9 (Nugent et al. 1981; Rutherford and Zimmermann 1984). This signal causes irregularities in the peak heights of lines 1, 2 and 3 of the MLS (for line numbering, see Figure 2). The light *minus* dark EPR spectrum induced by excitation of membrane fragments with a single light flash at T = 273K and subsequent rapid freezing (spectrum not shown) shows also the MLS and the g = 4.1 signal with only slightly changed relative intensities in favor of the MLS.

The MLS of PS II membrane fragments and PS II core complexes recorded at 10 K is depicted in an expanded view in Figure 2. A high field modulation depth of 2.0 mT was used to obtain maximum signal intensities. Values of 1.0 mT or even 0.5 mT did not lead to better resolved spectra. For a detailed discussion of the S_2 MLS features the lines are numbered as indicated in Figure 2a. Figures 2a and 2b compare the MLS (light *minus* dark) of membrane fragments generated by a single light flash at 273 K and by continuous illumination at 200 K, respectively. In the former case the $Fe^{2+}Q_A^{-\bullet}$ signal does not contribute to the spectrum (see effect on lines 1 to 3). Apart from this effect, the two spectra are strikingly similar with respect to line positions, line spacings and line splittings. The observed number of major lines in Figure 2a is 18 (9 on each side from the center). One additional line is obscured by the strong radical species at g = 2.00 yielding 19 lines in total. The line spacing is 8.0 to 9.0 mT. The same holds for the spectrum in Figure 2b but lines 9 and −9 do not clearly show up. Most of the EPR lines do not exhibit any splitting whereas the lines −3 and −1 show a shoulder and a splitting is indicated on lines 2, 3 and 4. The lines −7, −8 and −9 of spectrum 2a show a pronounced structure that possibly can be explained by an additional hyperfine splitting of these lines. This feature is, however, not clearly present in the other spectra of the MLS. In general, the line splittings in the high field region are more pronounced than in the low field region of the MLS.

Figures 2c and 2d compare the MLS of core complexes generated either by continuous illumination (2c) or flash excitation (2d) as described for the PS II membrane fragments. A closer inspection of the two spectra shows that they are almost identical. The number of lines is 19 and the line spacings are 8.0 to 9.0 mT. Comparison with the same signals from PS II membrane fragments (2a, 2b) reveals a strong similarity showing

that the part of the water oxidizing site giving rise to the MLS is the same in both kinds of preparations. In both spectra (2c, 2d) the $Fe^{2+}Q_A^{-\bullet}$ signal is absent. This is in agreement with the recent observation that a strong narrow $Q_A^{-\bullet}$ EPR signal (g = 2.0047) is observed in this preparation (Adir et al. 1992; MacMillan et al. 1995) which shows that $Q_A^{-\bullet}$ is decoupled from the non-heme iron in the core complexes.

In Figure 3 the EPR spectra of dark adapted PS II core complexes are shown before and after continuous illumination at T = 200K. The spectrum of the dark adapted sample exhibits several signals associated with PS II (Figure 3a). The signal near g = 6 can be assigned to the perpendicular component of cytochrome *b*-559 with the heme iron (Fe^{3+}) being in the high spin form (Shuvalov et al. 1995, and references therein). The splitting of this signal indicates a slight deviation from axial symmetry. The low spin counterpart of cytochrome *b*-559, that is also present, displays an EPR signal with components at $g_1 = 3.0$ and $g_2 = 2.3$. The expected third component at about $g_3 = 1.5$ is usually quite broad and is not detected here. These signals arising from the high and low spin heme in Cyt *b*-559 are *not* present in PS II membrane fragments under the same experimental conditions. Another marked feature in this spectrum is the signal at g = 4.3 that is ascribed to a rhombic iron Fe^{3+} species. The origin of this species is still unknown although it appears in all types of PS II preparations and under all conditions investigated so far.

The five lines centered arround g = 2 are part of the EPR spectrum of the Mn^{2+} hexaquo complex which is formed by manganese ions that are released from the WOC during the isolation procedure of the PS II core complexes. These manganese ions are still loosely bound to the protein. The sixth line of this signal is obscured by the EPR signal of tyrosine Y_D^{ox} which is not shown in the spectra. The same sample after illumination at 200K shows the spectrum in Figure 3b. The g = 4.1 signal and the MLS appear while the other signals are virtually not influenced by light.

Figure 3c shows the light *minus* dark difference spectrum (b–a) yielding the light-induced EPR signals. Since no photochemistry is expected to take place involving the rhombic Fe^{3+} the subtraction is carried out in such a way that this signal at g = 4.3 disappears completely. However, this procedure does not completely eliminate the cytochrome b-559 signal at g = 6 (see Figure 3c). This is due to the fact that the saturation behavior and thereby the amplitude of the different Fe signals are strongly dependent on temperature. Even very small temperature differences during recording of the dark and the light spectrum can thus result in drastic relative amplitude changes. Therefore, not all iron signals disappear completely when the spectra are normalized to the rhombic iron signal. Note that this can also lead to a distortion of the MLS caused by contributions of the Mn^{2+} signal (compare Figure 2d). It is remarkable that in the core complexes the S_2 state shows the g = 4.1 signal. The relative amplitudes of the g = 4.1 and the MLS are similar to those observed for membrane fragments (compare Figure 1).

ENDOR measurements

In order to obtain information on the interaction of the electron spin of the WOC with the ligand environment we have performed ^{1}H-ENDOR experiments on the MLS. For these experiments core complexes were chosen in which a better signal-to-noise ratio was achieved and two additional hf splittings could be resolved (for our earlier results on PS II membrane fragments, see Zweygart et al. 1992). To avoid contributions from the strong signals near g = 2 the experiments have been performed at different field positions (position A and B marked in Figure 2d) that are equivalent to g-values of 2.28 and 1.89, respectively. These positions are sufficiently far apart from the strong signal near g = 2; i. e. −37 mT for position A and 24 mT for position B. However, interference with other radical species with rather broad EPR spectra cannot be excluded (see Figure 3).

In order to check for signals that are not related to redox state S_2 of the WOC, ENDOR spectra were measured in samples where the WOC was kept in the EPR silent S_1 state. Figures 4a and 4b show the ^{1}H-ENDOR spectra obtained in dark adapted PS II core complexes that were suspended in H_2O buffer. The spectrum in Figure 4a (position A) exhibits four hyperfine splittings: a narrow feature with 0.6 MHz, a proton matrix line with 1.1 MHz, a shoulder with 1.7 MHz and a large splitting with 3.3 MHz. At line position B (Figure 4b) a similar ENDOR spectrum is obtained but with at least three times less intensity. In the latter case only the matrix peak and the large component with 3.3 MHz can be unambiguously assigned. The origin of the ENDOR signals in dark adapted samples depicted in Figures 4a and 4b will not be analyzed in this study because they do not provide information on the interaction of protons with the manganese cluster.

Upon generation of the S_2 state by cw illumination at T = 200K ENDOR signals are observed as shown

in Figures 4c and 4d. These ENDOR spectra of illuminated PS II core complexes are expected to contain contributions from both the S_2 state of the WOC and other species not related to the manganese cluster. If one assumes that the latter contributions are invariant to illumination, the ENDOR spectrum of S_2 should be obtained as the difference of the signals measured in illuminated and dark adapted samples. The difference spectra are depicted in Figures 4e and 4f. They exhibit hfc's of 0.6 MHz, 1.1 MHz, 2.3 MHz and 4.2 MHz. The value of the largest coupling of 4.2 MHz is slightly reduced to 4.0 MHz if one assumes a derivative line form (see also Table 1). These signals could originate either from exchangeable or non-exchangeable protons. In the case of water bound to the WOC the protons should be exchangeable and, therefore, should disappear in samples suspended in D_2O buffer.

D_2O exchange does not alter the EPR spectra of PS II because they are governed by the hyperfine couplings of the manganese nuclei and are hardly influenced by the ligand sphere. This was indeed found to be the case. The ^{1}H-ENDOR spectra for the dark adapted state of core complexes suspended in D_2O are virtually the same as those of sample in H_2O (spectra not shown). The light induced samples exhibit, however, pronounced differences. In order to illustrate this effect, difference ^{1}H-ENDOR spectra were monitored. The results depicted in Figures 4g and 4h reveal that all lines that were present in the spectra 4e and 4f are markedly reduced in their amplitudes. Therefore, the related hfc's reflect exchangeable protons that interact with the manganese cluster in the S_2 state of the WOC whereas the hfc's detected in the dark adapted state are assigned to other paramagnetic species.

Discussion

The multiline signal

The broad and highly structured multiline signal centered around g = 2 is characteristic for the S_2 state of the WOC. This typical signal is observed in different types of PS II preparations isolated from either cyanobacteria or higher plants (for a review, see Debus 1992). Most of the former studies were performed on PS II enriched membrane fragments but the MLS can be also observed in spinach chloroplasts (Dismukes and Siderer 1980; Brudvig et al. 1983). The MLS has been observed in PS II core complexes from spinach (Sivaraja and Dismukes 1988) and recently from the cyanobacterium *Synechocystis* PC 6803 (Tang and Diner 1994). These PS II core preparations contain only one of the extrinsic regulatory proteins, i.e. the *psb*O gene product, designated as extrinsic 33 kDa protein. It therefore seems worth analyzing the possible effect of other extrinsic proteins on the properties of the manganese cluster in the WOC. EPR measurements provide a useful tool to analyze this problem. However, signals from different investigations can hardly be compared because of the widely different conditions that were used, e.g. the buffer composition, EPR experimental conditions etc. To our knowledge, there exists only one report that presents a direct comparison between different preparations and different excitation procedures (Sivaraja and Dismukes 1988). In the present paper an extented comparative analysis has been presented.

Figure 2 shows spectra of the MLS of PS II membrane fragments and core complexes, both illuminated at low temperature (T = 200 K) and at T = 273 K. The number of lines is 19, although the outermost lines (9, −9) are weak and sometimes hardly detectable (Figure 2b) and the center line is superimposed by the Y_D^{ox} signal. Regardless of this particular problem the number of major lines and their spacings remain largely unchanged in the different preparations and under the different conditions used here. The striking similarity of the multiline signals from PS II membrane fragments and from core complexes illuminated either at low temperature (Figures 2b and 2d) or by a flash at 273 K (Figures 2a and 2c) provides valuable information on the interaction of the WOC with the protein subunits of PS II. The core complexes are lacking the 17 and 23 kDa proteins that are present in membrane fragments from higher plants. Therefore, the EPR spectra presented in Figure 2 conclusively show that these extrinsic proteins do not influence the hyperfine interaction of the manganese and the integrity of the metal cluster. On the other hand, the additional removal of the 33 kDa protein from PS II membrane fragments affects the structure of the MLS (Fiege et al. 1995).

Further information on the S_2 state of the WOC can be gained from the analysis of the hyperfine structure of the MLS. It was found that S-band EPR spectra (3.9 GHz) of the MLS exhibit several additional lines compared with X-band spectra that are due to second and/or higher order effects (Haddy et al. 1990). These effects give rise to a line splitting pattern that is *more* pronounced in the high field region. In this respect it is worth mentioning that the X-band MLS also exhibits a better resolution of the lines in the high-field as compared with the low-field region (see Figure 2). Inter-

estingly, in the spectra of Mn(III)Mn(IV) model complexes a similar feature is observed. This was explained by a combination of g- and hyperfine anisotropy with a particulary large Mn(III) hf anisotropy (Zweygart 1995). It is tempting to assume a similar situation for the WOC to explain this characteristic feature of the MLS.

The g = 4.1 signal

The nature of the g = 4.1 signal is still a matter of discussion (for a review, see Debus 1992). This signal might arise from a higher spin state (S = 3/2) of the exchange coupled manganese cluster (Smith et al. 1993). In both of our preparations this signal is present irrespective of the conditions of its light-induced formation. The presence of the g = 4.1 signal in the EPR spectra of the PS II core complexes (Figure 3c) shows that the absence of the extrinsic 17 and 23 kDa proteins does not result in a loss of the g = 4.1 signal. This is in contrast to PS II preparations from cyanobacteria that lack these two subunits *and* the g = 4.1 signal. (McDermott et al. 1988). A loss of the g = 4.1 signal was also reported for PS II membrane fragments from spinach deprived of the 17 and 23 kDa proteins by NaCl washing and subsequent Cl^- replacement (de Paula et al. 1986). In analogy to the significant reduction of the 4.1 signal in Ca^{2+} depleted PS II membrane fragments by low pH treatment (Ono et al. 1991) the presence of Cl^- might be essential for the formation of the 4.1 signal. So far we could not detect the g = 4.1 signal in PS II preparations lacking the 33 kDa protein. We conclude that the presence of the 33 kDa protein might be necessary for formation of the g = 4.1 signal while a modified MLS can be observed even in the absence of this subunit (Fiege et al. 1995).

ENDOR

The ENDOR spectra exhibit several splittings in the dark adapted state and some additional lines after light excitation. The resulting hfc's are summarized in Table 1 and compared with those of other studies. The comparison of the hf splittings of the dark adapted sample with those of the S_2 state clearly shows that splittings which are present in the dark state (1.7 and 3.3 MHz) are absent in the light *minus* dark difference spectra. Furthermore, at least two new splittings arise in the S_2 state (2.3 and 4.0 MHz). These hfc's should give valuable information on protons in the environment of the WOC. It is important to note that these lines are diminished in amplitude or even disappear in samples that were suspended in D_2O instead of H_2O.

The hf splittings found by Kawamori et al. (1989) and Zweygart et al. (1992) in PS II membrane fragments from spinach, and by Tang et al. (1993) in PS II core complexes from the cyanobacterium *Synechococcus elongatus* are also given in Table 1. The small differences between the hfc's can be explained by the error arising from the rather poor signal-to-noise ratio of all spectra and probably also by differences in samples or species. Nevertheless, some structural information can be gathered from these hf data. Kawamori et al. (1989) estimated a closest manganese to proton distance of 2.7 Å (2.4 Å) using the simple point-dipole model leading to Eq. (2) and a spin density at the manganese of 1.0 (0.5). In contrast, Tang et al. (1993) considered the possibility of a rhombic hf tensor assigned to the three largest couplings of 4.9, 2.4 and 1.0 MHz and estimated a proton manganese distance of 3.8 Å.

Based on a simple point-dipole model the hf components of S_2 obtained in the present study can either represent the parallel or the perpendicular component of an axial tensor. The parallel component $A_{||}$ could be rather broad and much less intense than the corresponding perpendicular component $A_\perp$ and may therefore not be detected in the spectra. This is supported by the analysis of ^{1}H-ENDOR spectra from Mn(III)Mn(IV) model complexes (Zweygart 1995).

Assuming that both line pairs belong to perpendicular components of two hfc tensors (Equation (2)) with $\rho = 1$ yields a proton-to-manganese distance of 3.3 Å for the 2.3 MHz and of 2.7 Å for the 4.0 MHz component.

The use of the modified point-dipole model given by Equation (6) leads to an alteration of the distances calculated from the same data set. This is caused by the fact that although one observes only an effective spin of the cluster, the ligand hf couplings are weighted sums of the interactions with the electronic spins of the individual metal ions. In order to illustrate this effect, a geometrical situation is assumed that is described by scheme 2 with ^{1}H either bound to Mn(III) or Mn(IV) (in both cases, $\psi = 0°$ in the calculation). Equation (9) describes this simplified case. The distance d between the two manganese is 2.7 Å in accordance with recent EXAFS data (Mukerji et al. 1994). This yields distances that depend upon the proton being located either on the Mn(III) or the Mn(IV) side. Keeping the assumption that the observed lines are $A_\perp$ components for a proton either on the Mn(IV) or the Mn(III) side distances of 2.5 Å or 3.3 Å, respectively, are obtained

Table 1. ^{1}H hyperfine splittings obtained from the multiline signal (S_2 state) by cw ENDOR spectroscopy

		Field pos.	Hyperfine splittings in MHz						Ref.
(1)	Dark	A	0.6^d		1.1^p	1.7^p	3.3^p		This work
(2)	Dark	B		0.8^p			3.2^p		This work
(3)	S_2	A	0.6^d		1.1^p		2.3^d	4.2^p/4.0^d	This work
(4)	S_2	B	0.6^d		1.1^p		2.3^d	4.2^p/4.0^d	This work
(5)	S_2		0.53	0.76	1.19	1.44	2.41	4.01	[1]
(6)	S_2			0.7			2.4		[2]
(7)	S_2		0.5		1.0		2.4	4.9	[3]

In rows (1) and (2) ENDOR splittings obtained from dark adapted PS II core complexes are given (see Figure 4a, b); (3) and (4) list the respective splittings obtained from the light *minus* dark difference spectra (see Figure 4e, f); ^{d,p} indicate the position on the line from which the hf splitting was obtained (d = derivative, p = peak), see filled circles in Figure 4; (5) to (7) show ENDOR data from other studies ([1] Kawamori et al. 1989, [2] Zweygart et al. 1992, [3] Tang et al. 1993).

for the 4.0 MHz component and distance of 2.9 Å or 3.9 Å, respectively, for the 2.3 MHz component.

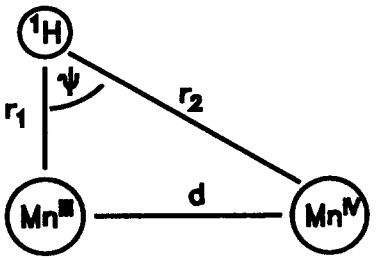

Scheme 3

As described above, the dipolar hf coupling tensor of a proton to a coupled electron spin system is not necessarily axial. For such a situation, it is very likely that only the component of the tensor with the largest statistical weight (central component) can be detected in an ENDOR spectrum with the given signal-to-noise ratio. Such a non-axial hf tensor is obtained if we assume a proton position as given in scheme 3. In that case a distance of 2.1 Å or 3.1 Å between the proton and Mn(IV) or Mn(III), respectively, results under the assumption that the 4.0 MHz hfc belongs to the central component. This would imply that the larger hf components of the tensor are broadened and beyond detection.

It is assumed that the observed exchangeable protons belong to water molecules and that they are ligated via their oxygen atoms to the manganese. The calculation of specific oxygen to manganese distances requires further structural assumptions and is therefore not performed here. The Mn-O distance is expected to be smaller than the Mn-H distances calculated from the ENDOR data. Typical distances of Mn(III,IV) to terminal ligands in various model complexes are 2.0 ± 0.1Å (Weyhermüller 1994). From our results it is therefore very well possible that water is *directly* ligated to the manganese nuclei of the WOC.

Acknowledgments

Financial support by Deutsche Forschungsgemeinschaft: 'Schwerpunktprogramm Bioanorganische Chemie' and 'Fonds der Chemischen Industrie' is gratefully acknowledged. Work at UCSD was supported by a grant from USDA (93-37306-9579).

References

Adir N, Okamura MY and Feher G (1992) Cristallization of the PSII-reaction center. In: Murata N (ed) Research in Photosynthesis, Vol II, pp 195–198. Kluwer Academic Publishers, Dordrecht, The Netherlands

Åhrling KA and Pace RJ (1995) Simulation of the S_2 state multiline electron paramagnetic resonance signal of Photosystem II: A multifrequency approach. Biophys J 68: 2081–2090

Babcock GT (1987) The photosynthetic oxygen-evolving process. In: Amesz J (ed) Photosynthesis, New Comprehensive Biochemistry, Vol 15, pp 125–158. Elsevier, Amsterdam

Berthold DA, Babcock GT and Yocum CF (1981) A highly resolved, oxygen-evolving Photosystem II preparation from spinach thylakoid membranes. FEBS Lett 134: 231–234

Bittl R (1993) Matrix elements of spin operators in exchange coupled tetrameric metal clusters. Chem Phys Lett 215: 279–284

Bonvoisin J, Blondin G, Gired J-J and Zimmermann J-L (1992) Theoretical study of the multiline EPR signal from the S_2 state of the oxygen evolving complex of Photosystem II. Biophys J 61: 1076–1086

Britt RD, Lorigan GA, Sauer K, Klein MP and Zimmermann J-L (1992) The g = 2 multiline EPR signal of the S_2 state of

the photosynthetic oxygen-evolving complex originates from a ground spin state. Biochim Biophys Acta 1140: 95–101

Brudvig GW, Casey JL and Sauer K (1983) The effect of temperature on the formation and decay of the nultiline EPR signal species associated with photosynthetic oxygen evolution. Biochim Biophys Acta 723: 366–371

de Paula JC, Li PM, Miller A-F, Wu BW and Brudvig GW (1986) Effect of the 17- and 23-kilodalton polypeptides, calcium, and chloride on electron transfer in Photosystem II. Biochemistry 25: 6487–6494

de Paula JC, Beck WF, Miller A-F, Wilson RB and Brudvig GW (1987) Studies of the manganese site of Photosystem II by electron spin resonance spectroscopy. J Chem Soc Faraday Trans 1 83: 3635–3651

Debus RJ (1992) The manganese and calcium ions of photosynthetic oxygen evolution. Biochim Biophys Acta 1102: 269–352

Debus RJ, Barry BA, Sithole I, Babcock GT and McIntosh L (1988a) Directed mutagenesis indicates that the donor to P_{680}^{+} in Photosystem II is tyrosine-161 of the D1 polypeptide. Biochemistry 27: 9071–9074

Debus RJ, Barry AB, Babcock GT and McIntosh L (1988b) Site-directed mutagenesis identifies a tyrosine radical involved in the photosynthetic oxygen-evolving system. Proc Natl Acad Sci USA 85: 427–430

Dismukes GC and Siderer Y (1980) EPR spectroscopic observations of a manganese center associated with water oxidation in spinach chloroplasts. FEBS Lett 121: 78–80

Fiege R, Zweygart W, Irrgang KD, Adir N, Geiken B, Renger G and Lubitz W (1995) EPR/ENDOR studies of the water oxidizing complex in Photosystem II. In: Mathis P (ed) Proceedings Xth Congress of Photosynthesis. Kluwer Academic Pubishers, Dordrecht, The Netherlands (in press)

Haag E, Irrgang KD, Boekema EJ and Renger G (1990) Functional and structural analysis of Photosystem II core complexes from spinach with high oxygen evolution capacity. Eur J Biochem 189: 47–53

Haddy A, Aasa R and Hansson Ö (1990) Low frequency (3.9 GHz) studies of the S_2-state EPR signals from the O_2-evolving complex, In: Baltscheffsky M (ed) Current Research in Photosynthesis, Vol I, pp 777–780. Kluwer Academic Publishers, Dordrecht, The Netherlands

Joliot P and Joliot A (1973) Different types of quenching involved in Photosystem II centers. Biochim Biophys Acta 305: 302–316

Kawamori A, Inui T, Ono T and Inoue Y (1989) ENDOR study on the position of hydrogens close to the manganese cluster in S_2 state of Photosystem II. FEBS Let 254: 219–224

Khangulov S, Sivaraja M, Barynin VV and Dismukes GC (1993) The dimanganese(III,IV) oxidation state of catalase from *Thermus thermophilus*: Electron nuclear double resonance analysis of water and protein ligands in the active site. Biochemistry 32: 4912–4924

Koike H and Inoue Y (1987) Temperature dependence of the S-state transition in a thermophilic cyanobacterium measured by thermoluminescence. In: Biggins J (ed) Progress in Photosynthesis Research, Vol I, pp 645–648. Martinus Nijhoff Publishers, Dordrecht, The Netherlands

Kurreck H, Kirste B and Lubitz W (1988) Electron Nuclear Double Resonance Spectroscopy in Solution. VCH, Weinheim

Kusunoki M (1992) A new paramagnetic hyperfine structure effect in manganese tetramers. The origin of 'multiline' EPR signals from an S_2 state of a photosynthetic water-splitting enzyme. Chem Phys Lett 197: 108–116

MacMillan F, Lendzian F, Renger G and Lubitz W (1995) EPR and ENDOR investigation of the primary electron acceptor radical anion $Q_A^{\bullet -}$ in iron-depleted Photosystem II membrane fragments. Biochemistry 34: 8144–8156

McDermott AE, Yachandra VK, Guiles RD, Cole JL, Dexheimer SL, Britt RD, Sauer K and Klein MP (1988) Characterization of the manganese O_2-evolving complex and the iron-quinone acceptor complex in Photosystem II from a thermophilic cyanobacterium by electron paramagnetic resonance and X-ray absorption spectroscopy. Biochemistry 27: 4021–4031

Messinger J and Renger G (1993) Generation, oxidation by the oxidized form of the tyrosine of polypeptide D2 and possible electronic configuration of the redox states S_0, S_{-1} and S_{-2} of the water oxidase in isolated spinach thylakoids. Biochemistry 32: 9379–9386

Messinger J, Schröder WP and Renger G (1993) Structure-function relations in Photosystem II. Effects of temperature and chaotropic agents on the period four oscillation of flash-induced oxygen evolution. Biochemistry 32: 7658–7668

Metz JG, Nixon PJ, Rögner M, Brudvig GW and Diner BA (1989) Direct alteration of the D1 polypeptide of Photosystem II: Evidence that tyrosine-161 is the redox component, Z, connecting the oxygen-evolving complex to the primary electron donor, P680. Biochemistry 28: 6960–6969

Miller A-F and Brudvig GW (1991) A guide to electron paramagnetic resonance spectroscopy of Photosystem II membranes. Biochim Biophys Acta 1056: 1–18

Mukerji I, Andrews JC, DeRose VJ, Latimer MJ, Yachandra VK, Sauer K and Klein MP (1994) Orientation of the oxygen-evolving manganese complex in a Photosystem II membrane preparation: An X-ray absorption spectroscopy study. Biochemistry 33: 9712–9721

Nugent JHA, Diner BA and Evans MCW (1981) Direct detection of the electron acceptor of Photosystem II. FEBS Lett 124: 241–244

Ono TA, Kusunoki M, Matsushita T, Oyanagi H and Inoue Y (1991) Structural and functional modifications of the manganese cluster in Ca^{2+}-depleted S_1 and S_2 states: Electron paramagnetic resonance and X-ray absorption spectroscopy studies. Biochemistry 30: 6836–6841

Pace RJ, Smith P, Bramley R and Stehlik D (1991) EPR saturation and temperature dependence studies on signals from the oxygen-evolving centre of Photosystem II. Biochim Biophys Acta 1058: 161–170

Renger G (1987) Mechanistic aspects of photosynthetic water cleavage. Photosynthetica 21: 203–224

Renger G (1992) Energy transfer and trapping in Photosystem II. In: Barber J (ed) The Photosystems: Structure, Function and Molecular Biology, pp 45–99. Elsevier, Amsterdam

Renger G (1993) Water cleavage by solar radiation – an inspiring challange of photosynthesis research. Photosynth Res 38: 229–247

Renger G, Gleiter HM, Haag E and Reifarth F (1993) Photosystem II: thermodynamics and kinetics of electron transport from Q_A^- to $Q_B(Q_B^-)$ and deleterious effects of copper(II). Z Naturforsch 48c: 234–240

Rutherford AW and Zimmermann JL (1984) A new EPR signal attributed to the primary plastoquinone acceptor in Photosystem II. Biochim Biophys Acta 767: 168–175

Shuvalov VA, Fiege R, Schreiber U, Lendzian F and Lubitz W (1995) EPR study of cytochrome in the D1D2 Cyt *b*-559 complex. Biochim Biophys Acta 1228: 175–180

Sivaraja M and Dismukes GC (1988) A comparison of the manganese center responsible for photosynthetic water oxidation in

O_2-evolving core particles and Photosystem II enriched membranes: EPR of the S_2 state. Isr J Chem 28: 103–108

Smith P, Ahrling KA and Pace RJ (1993) Nature of the S_2 state electron paramagnetic resonance signals from the oxygen-evolving complex of Photosystem II: Q-band and oriented X-band studies. J Chem Soc Faraday Trans 89: 2863–2868

Tang X-S and Diner BA (1994) Biochemical and spectroscopic characterization of a new oxygen-evolving Photosystem II core complex from the cyanobacterium *synechocystis* PCC 6803. Biochemistry 33: 4594–4603

Tang XS, Sivaraja M and Dismukes GC (1993) Protein and substrate coordination to the manganese cluster in the photosynthetic water oxidizing complex: ^{15}N and ^{1}H ENDOR spectroscopy of the S_2 state multiline signal in the thermophilic cyanobacterium *synechococcus elongatus*. J Am Chem Soc 115: 2382–2389

Vermaas WFJ, Rutherford AW and Hansson Ö (1988) Site-directed mutagenesis in Photosystem II of the cyanobacterium *Synechocystis* sp. PCC 6803: Donor D is a tyrosine residue in the D2 protein. Proc Natl Acad Sci USA 85: 8477–8481

Völker M, Ono T, Inoue Y and Renger G (1985) Effect of trypsin on PS-II particles. Correlation between Hill-activity, Mn-abundance and peptide pattern. Biochim Biophys Acta 806: 25–34

Weyhermüller T (1994) Synthese und Charakterisierung oxoverbrückter Mangankomplexe mit Azamakrozyklen – Modelle für das Photosystem II? Doctoral Thesis, Ruhr-Universität Bochum, Germany

Zheng M and Dismukes GC (1992) Photosynthetic water oxidation: What have we learned from the multiline EPR signals? In: Murata N (ed) Research in Photosynthesis, Vol II, pp 305–308. Kluwer Academic Publishers, Dordrecht, The Netherlands

Zweygart W (1995) ESR und ENDOR– Untersuchungen an mehrkernigen gemischtvalenten Mangankomplexen als Modelle für das wasseroxidierende Enzymsystem im Photosystem II. Doctoral Thesis, Technische Universität Berlin, Germany

Zweygart W, Weyhermüller T, Renger G, Wieghardt K and Lubitz W (1992) EPR and ENDOR studies of manganese clusters in the water-oxidizing complex. In: Murata N (ed) Research in Photosynthesis, Vol II, pp 289–292. Kluwer Academic Publishers, Dordrecht, The Netherlands

Zweygart W, Thanner R and Lubitz W (1994) An improved TM_{110} ENDOR cavity for the investigation of transition metal complexes. J Magn res, ser A 109: 172–176